

Disorder-induced superconducting ratchet effect in nanowires

S. Poran, E. Shimshoni, and A. Frydman

Department of Physics, Bar-Ilan University, Ramat Gan 52900, Israel

(Received 28 June 2011; published 29 July 2011)

A dc voltage drop develops along amorphous indium oxide wires that are exposed to an ac bias source. This voltage is antisymmetric with the magnetic field and is characterized by sample specific quasiperiodic magnetovoltage oscillations. The voltage magnitude increases with decreasing temperature below T_C but saturates at low T . As the disorder of the sample is decreased, the dc voltage is suppressed. This rectification is attributed to a superconducting ratchet effect in which disorder and geometrical confinement play the role of asymmetric pinning centers. This effect demonstrates the importance of inherent inhomogeneity and vortex motion in both sides of the superconductor-insulator transition of disordered superconductors.

DOI: [10.1103/PhysRevB.84.014529](https://doi.org/10.1103/PhysRevB.84.014529)

PACS number(s): 74.78.Na, 73.21.Hb, 74.25.Wx, 74.81.Bd

I. INTRODUCTION

Asymmetric pinning centers in superconducting films give rise to a ratchet effect in which vortices acquire a net motion in the presence of an ac driving force with time average zero. The potential exerts a counterforce with different magnitude for each direction of the driving force leading to a net velocity of vortices,^{1,2} thus rectifying an applied ac current to produce a dc voltage in a similar way to that of a diode. This effect has been demonstrated experimentally in superconductors in which a periodic asymmetric potential array such as triangular magnetic dots,³ asymmetric antidots,^{4,5} or Josephson junctions⁶ were fabricated. Similarly, ac current rectification has been shown to result from the edge effect in which geometrical imperfections of a superconductor's edge make it easier for a vortex to enter one side of the film than the other.⁷⁻⁹ In this paper we demonstrate a different type of ratchet effect that is achieved in disordered superconducting wires without the need to introduce geometrical asymmetry. We suggest that this effect can be utilized to study and shed light on the superconductor-insulator transition in disordered superconductors.

II. EXPERIMENT

Amorphous indium oxide films undergo a superconductor-insulator transition (SIT) as a function of disorder that can be controlled by low-temperature annealing.¹⁰ Despite the fact that the films are amorphous and are relatively uniform structurally,¹¹ there have been experimental observations that indicate that the electronic structure is inherently inhomogeneous on rather large length scales ($\leq 1 \mu\text{m}$). Two examples of this are a SIT as a function of the length in a set of amorphous InO short samples¹² and local scanning tunneling microscopy measurements showing spatial variations of the order parameter in InO films.¹³ Indeed, electronic granularity has been predicted to emerge in homogeneous disordered superconductors by a number of groups.¹⁴⁻¹⁷ Such inhomogeneity can be expected to have an especially large impact in low-dimensional systems in which at least one of the spatial extents is smaller than the scale of granularity.

The samples used in this study were lithographically defined InO nanowires, 30 nm thick, 40–90 nm wide, and 1–5 μm long. The InO was E-gun evaporated in a vacuum

chamber with a base pressure down to 1×10^{-7} mbar in which a partial oxygen pressure up to 1×10^{-4} mbar was introduced to produce samples with different initial disorder. The disorder was further reduced by vacuum annealing within the measurement probe at $T = 80^\circ\text{C}$ causing a continuous slow decrease of the wire resistance. The normal state resistance of the wires at $T = 10$ K ranged between 1 M Ω and 10 k Ω . We have studied 14 such wires at different degrees of disorder in the vicinity of the SIT, all showing the same qualitative behavior described below. Similar wires produced by a different technique were studied by Johansson *et al.*¹⁸ These wires exhibited low-temperature reproducible magnetoresistance oscillations. Here we focus on the response of the highly disordered wires to an external ac bias in a regime where these oscillations are suppressed.

III. RESULTS AND DISCUSSION

Throughout the experiment, an ambient radiation of 15.5 MHz, 0.02 mW was incident on the wires. Under these conditions even the most ordered wires did not reach a zero-resistance state at low T . Figure 1 shows the resistance versus temperature for a series of wires having different degrees of disorder that are characterized by the sheet resistance R_{sq} . It is seen that the wires undergo a disorder-driven SIT. However, even on the superconducting side of the transition the wire resistance saturates at a low-temperature residual resistance R^* , which increases with increasing disorder (or R_{sq} ; see the inset). Interestingly, also on the insulating side the resistance seems to be approaching a finite R^* rather than increasing exponentially with lowering T . Two-dimensional films prepared with the same disorder as these wires always shows full superconductivity even in the presence of an induced ac bias, as demonstrated in the inset of Fig. 1.

The observed finite resistance is not surprising. The superconducting coherence length ξ in disordered indium oxide films is 10–30 nm,¹⁸ which is not much smaller than the width of our wires. One can expect the imposed ac force to induce phase slips or vortex-antivortex motion, which would generate dissipation in the wire (though the temperature dependence needs clarification). A feature that is much less expected is the appearance of a dc voltage along the wire that is antisymmetric with magnetic field. Figure 2 depicts a magnetovoltage $[V(H)]$

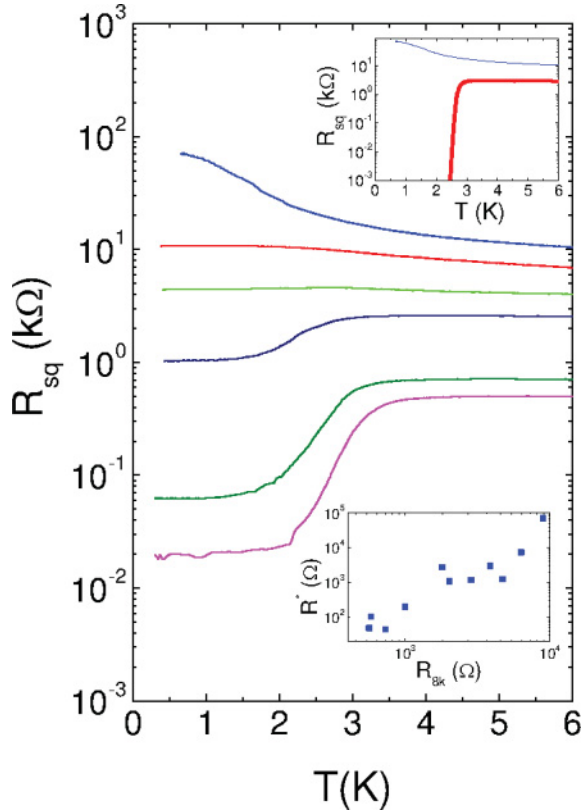


FIG. 1. (Color online) Resistance versus temperature for a number of InO wires with different R_{sq} . The top inset shows $R(T)$ of a film with dimensions $1\text{ mm} \times 1\text{ mm}$ (heavy red line) and a $1\text{-}\mu\text{m} \times 50\text{-nm} \times 30\text{-nm}$ nanowire (light blue line) having the same disorder. The bottom inset shows the residual resistance R^* as a function of the normal state sheet resistance.

curve of a $1\text{-}\mu\text{m}$ -long wire. This voltage is measured by a Keithley 2182A nanovoltmeter connected to the two ends of the wire without any driving current. It is seen that the voltage increases rapidly up to a field H_m at which point it reaches a maximal value V_m . For $H > H_m$ the voltage decreases gradually. This qualitative behavior is seen for all measured wires including those on the insulating side of the SIT. Figure 2 also shows that, for our wires, an additional fine structure is superimposed on the overall $V(H)$ curve. These features are sample dependent but are easily reproducible in a single wire even after repeated thermal cycling and show nearly perfect antisymmetric behavior $V(H) = -V(-H)$. Fourier transforming the $V(H)$ curves of our wires yields a dominant quasiperiod that corresponds to a magnetic field of $0.6\text{--}1.5\text{ T}$. This is consistent with a magnetic flux quantum penetrating a loop of diameter of $20\text{--}50\text{ nm}$, which is close to the width of our wires. Hence it seems reasonable to attribute each quasio oscillation to an additional vortex penetrating the wire. None of these features was seen in the magnetoresistance of the wires, measured by standard lock-in techniques, which showed a steady increase of resistance with increasing magnetic field up to 6 T .

A rectification of an ac driving force that is antisymmetric with H is an identifying trait of the ratchet effect of vortex motion. The unique feature observed in our wires is the dependence of the rectified voltage on disorder. Figure 3(a)

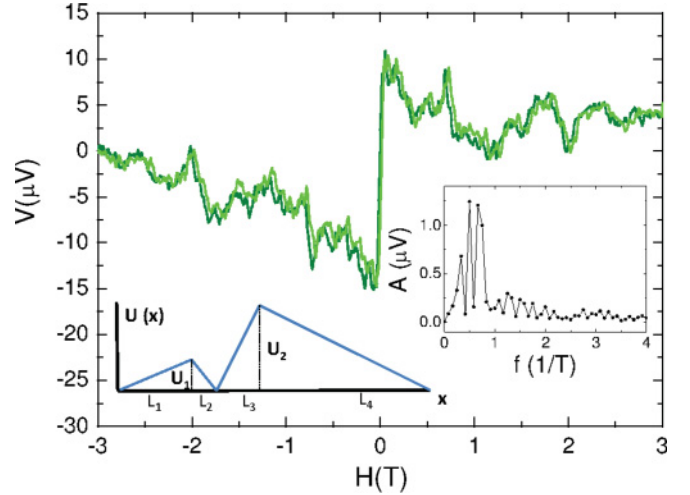


FIG. 2. (Color online) dc voltage as a function of magnetic field for a $1\text{-}\mu\text{m} \times 30\text{-nm} \times 50\text{-nm}$ InO wire. The two curves are a trace and a retrace showing that the fine structure is easily reproducible. The right inset shows the Fourier transform of the curve after subtracting the main feature background. The left inset is a schematic illustration of the pinning potential $U(x)$ along the superconductor's cross section.

depicts $V(H)$ of a single $1\text{-}\mu\text{m}$ -long nanowire for three annealing stages near the SIT. It is seen that the dc voltage exhibits a monotonic decrease upon reducing the disorder, quantified by R_{sq} . Such a disorder dependence is not expected for the conventional ratchet effect that is based on geometrical asymmetry (either of pinning sites or of edges) in clean superconductors. Apparently, disorder plays an important role in the ratchet effect of our wires in which geometrical asymmetry is not intentionally introduced. As mentioned above, the highly disordered wires may be characterized by inherent inhomogeneity. Hence they may include regions of normal metal or weak superconductivity that act as pinning centers for vortices. The geometry of the wire, in which the width is not much larger than the scale of inhomogeneity, gives rise to a natural asymmetry of pinning centers that are closer to one edge of the wire than the other. This interplay between disorder and wire geometry makes it easier for a vortex to cross the barrier to one side than to the other, thus producing a unique rectification effect.

A simple model for the pinning profile across the wire $U(x)$ due to a single pinning site placed asymmetrically with respect to the width of the wire is illustrated in the inset of Fig. 2. Here the superconducting regions within the wire act as barriers for vortices and the normal insulators outside the wire are vortex reservoirs. A vortex in the potential well is subject to an ac driving force with amplitude $f_d = j_{ac}\Phi_0 d/c$, where j_{ac} is the ac current density, $\Phi_0 = 2 \times 10^{-7}\text{ G cm}^2$ is the flux quantum, and d is the film thickness. For small amplitudes of driving force $f_d \ll \frac{dU}{dl}$, with l being the barrier length, the dc voltage V is proportional to the difference between the probabilities to cross over the barriers:

$$V \propto e^{-(U_1 - f_d l_2)/k_B T} - e^{-(U_2 - f_d l_1)/k_B T}, \quad (1)$$

where U_1 and U_2 are the potential barriers for a vortex to escape the wire in either direction.

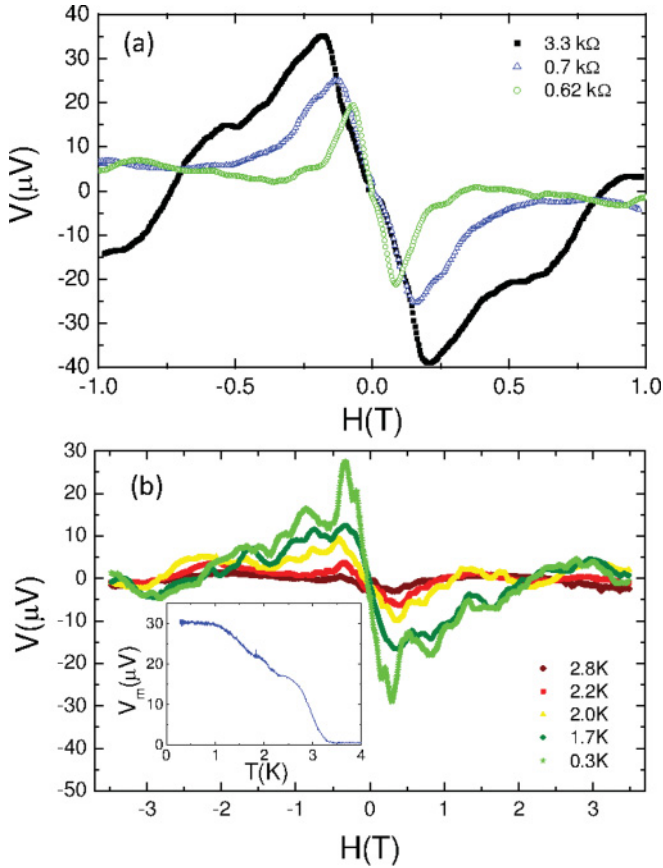


FIG. 3. (Color online) (a) $V(H)$ curves for a $1\text{-}\mu\text{m} \times 30\text{-nm} \times 50\text{-nm}$ InO wire for three stages of disorder, achieved by thermal annealing. (b) $V(H)$ curves for a different $1\text{-}\mu\text{m} \times 30\text{-nm} \times 50\text{-nm}$ InO wire measured at various temperatures. The inset shows the maximal voltage V_m as a function of temperature.

Equation (1) predicts that V should increase with increasing disorder, which would increase the relevant potential barriers, and with decreasing temperature. Both these trends are observed in our wires. The effect of disorder, depicted in Fig. 3(a), was discussed above. The temperature dependence of $V(H)$ for a typical wire is shown in Fig. 3(b). It is seen that below T_C the curve increases in amplitude with lowering T , as expected from Eq. (1). However, below a characteristic temperature \tilde{T} the voltage saturates and becomes temperature independent, as seen in the inset of Fig. 3(b). In all our wires \tilde{T} is found to be between 1.3 and 2 K and is very close to the temperature at which the resistance reaches the saturation value R^* (Fig. 1). The saturation of $V(T)$ may be attributed to a crossover from thermal excitation of the vortices' motion to quantum tunneling through the barriers. Such interpretation clearly requires a detailed theoretical treatment and further experimental investigation.

When the driving force is increased so that it approaches the force exerted by the pinning potential, the barrier is suppressed and the exponential activation form of Eq. (1) does not apply. The vortices become free and their motion can be described by a viscous flow.¹ For each pinning center, having a potential profile such as that illustrated in the inset of Fig. 2, the velocity

due to the viscous flow that is proportional to the rectified voltage can be shown to be given by

$$v = \begin{cases} 0 & \text{for } f_d < f_2 \\ \frac{1}{2\eta} \frac{(f_d + f_1)(f_d - f_2)}{f_d + f_1 - f_2} & \text{for } f_2 < f_d < f_3 \\ \frac{1}{2\eta} \frac{(f_d + f_1)(f_3 - f_2)f_1}{(f_d + f_1)(f_d + f_1 - f_2 - f_3) + f_2 f_3} & \text{for } f_3 < f_d, \end{cases} \quad (2)$$

where $f_2 = \frac{U_1}{L_2}$, $f_3 = \frac{U_2}{L_3}$, and $f_1 = \frac{U_1}{L_1} = \frac{U_2}{L_4}$ are the forces generated by the pinning potential and η is the viscous drag coefficient for vortex motion.

Equation (2) describes a nonmonotonic dependence of the vortex velocity on the magnitude of the ac driving current. The reason for this is that when the driving force is very low, vortex motion is limited for both bias orientations and when it is very high it will generate equivalent vortex motion in both directions. Thus the voltage reaches a maximum at intermediate force amplitude $f_d = f_3$ and is very small for both high and low f_d amplitudes. In our wires the voltage may be governed by a number of pinning sites, each characterized by a different potential profile and contributing differently to the total voltage drop. In this case the dependence of voltage on applied ac current magnitude can be nontrivial and include a number of maxima. In order to study the effect of the ac force amplitude we applied an external ac power with variable power and frequency on our wire. Figure 4 shows the rectified voltage along a $5\text{-}\mu\text{m}$ -long wire as a function of the applied ac bias power P and frequency f . Here the background effect due to the 15-MHz ambient radiation was subtracted.¹⁹ A number of points should be noted. First, there is a threshold ac power P_{\min} below which no voltage is detected (P_{\min} is frequency and magnetic field dependent). Second, the voltage is nonmonotonic with ac power and shows a series of peaks. Third, depending on the magnetic field, the voltage can be either positive or negative. At certain magnetic fields the voltage may change sign as a function of bias power, thus manifesting a ratchet reversal effect.³ This

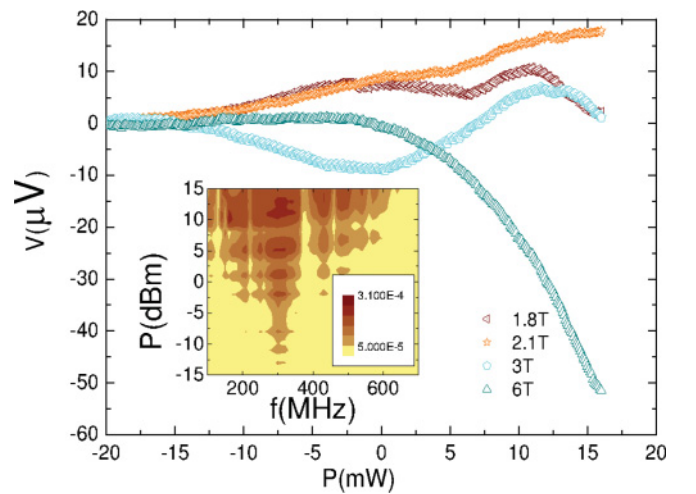


FIG. 4. (Color online) dc voltage as a function of 100-kHz power for a $5\text{-}\mu\text{m}$ -long InO wire measured at different magnetic fields, which correspond to peaks on the $V(H)$ curve. The background voltage due to the ambient radiation was subtracted from these measurements. The inset shows the voltage as a function of power and frequency at $H = 2.4$ T.

behavior reflects the summation of contribution from a number of vortex pinning sites, each one having different asymmetry and hence a specific ac power and magnetic field dependence of voltage magnitude and sign. Finally, we note that there is a cutoff frequency $f_{CO} \sim 600$ MHz, above which no ratchet voltage is detected. This is indeed expected¹ when the driving force change is too fast to allow the asymmetric motion of vortices. Interestingly, the low-temperature residual resistance R^* has a similar dependence on P to that of the rectified voltage.²⁰

The longer the wire, the more pinning centers can be expected to contribute. The total voltage is given by $V = \sum V_i$, where V_i , the contribution of pinning site i , is random in size and can be either positive or negative and V is the sum of random numbers and is expected to increase in magnitude like $V \propto \sqrt{N}$ (where N is the number of sites generating a random voltage). Increasing the wire length should lead to a richer structure of $V(f_a)$ and to larger V . We measure two 5- and twelve 1- μm -long wires. The former yield voltages that are more than twice as large as the average voltage measured in the latter having equivalent disorder. The longer wires also show a richer and more prominent fine structure as a function of magnetic field and ac bias power. The opposite trend can be expected with increasing wire width. The ratchet effect should be suppressed when the width exceeds the scale of inhomogeneity. Indeed, we do not detect any dc voltage for wires having widths of several micrometers. A detailed study

of the dc voltage dependence on wire length and width is beyond the scope of the present paper.²⁰

IV. CONCLUSION

In summary, this work suggests a type of superconducting ratchet effect in which there is no need for intentional geometric asymmetry. This effect is maximized in the critical regime close to a SIT, which is a regime that presently lacks a satisfactory theoretical understanding. Hence the disorder-tuned rectification not only demonstrates the possibility of a spontaneous ratchet effect, but can also be viewed as an interesting probe for the vortex dynamics in this critical regime. The results of this work provide a clear illustration of the significance of inherent electron inhomogeneity in driving the SIT of these materials. In particular they demonstrate that vortices are instrumental in the processes that lead to dissipation and electric resistance in disordered superconductors and are present even on the insulating side of the transition.

ACKNOWLEDGMENTS

We are grateful for useful discussions with C. Bolech, Z. Ovadyahu, G. Refael, and N. Shah. This research was supported by the United States–Israel Binational Fund (Grant No. 2008299). E.S. acknowledges support from the Israel Science Foundation (Grant No. 599/10) and from the Israeli Ministry of Science and Technology (Grant No. 3-5792).

¹C. S. Lee, B. Janko, I. Derenyi, and A. L. Barabasi, *Nature (London)* **400**, 337 (1999).

²For a review see B. L. T. Plourde, *IEEE Trans. Appl. Supercond.* **19**, 3698 (2009), and references cited therein.

³J. E. Villegas, S. Savelev, F. Nori, E. M. Gonzalez, J. V. Anguita, R. Garcia, and J. L. Vicent, *Science* **302**, 1188 (2003).

⁴C. C. de Souza Silva, J. Van de Vondel, M. Morelle, and V. V. Moshchalkov, *Nature (London)* **440**, 651 (2006).

⁵B. B. Jin, B. Y. Zhu, R. Wördenweber, C. C. de Souza Silva, P. H. Wu, and V. V. Moshchalkov, *Phys. Rev. B* **81**, 174505 (2010).

⁶D. E. Shalóm and H. Pastoriza, *Phys. Rev. Lett.* **94**, 177001 (2005).

⁷D. Y. Vodolazov and F. M. Peeters, *Phys. Rev. B* **72**, 172508 (2005).

⁸F. G. Aliev, *Physica C* **437**, 1 (2006).

⁹S. A. Harrington, J. L. MacManus-Driscoll, and J. H. Durrell, *Appl. Phys. Lett.* **95**, 022518 (2009).

¹⁰D. Shahar and Z. Ovadyahu, *Phys. Rev. B* **46**, 10917 (1992).

¹¹A. F. Hebard and S. Nakahara, *Appl. Phys. Lett.* **41**, 1130 (1982).

¹²D. Kowal and Z. Ovadyahu, *Solid State Commun.* **90**, 783 (1994); *Physica C* **468**, 322 (2008).

¹³B. Sacepe, T. Dubouchet, C. Chapelier, M. Sanquer, M. Ovadia, D. Shahar, M. Feigelman, and L. Ioffe, *Nature Phys.* **7**, 239 (2011).

¹⁴N. Trivedi, R. T. Scalettar, and M. Randeria, *Phys. Rev. B* **54**, R3756 (1996); A. Ghosal, M. Randeria, and N. Trivedi, *ibid.* **65**, 014501 (2001).

¹⁵E. Shimshoni, A. Auerbach, and A. Kapitulnik, *Phys. Rev. Lett.* **80**, 3352 (1998).

¹⁶Y. Dubi, Y. Meir, and Y. Avishai, *Phys. Rev. B* **73**, 054509 (2006); *Nature (London)* **449**, 876 (2007).

¹⁷Y. Imry, M. Strongin, and C. C. Homes, *Physica C* **468**, 288 (2008).

¹⁸A. Johansson, G. Sambandamurthy, D. Shahar, N. Jacobson, and R. Tenne, *Phys. Rev. Lett.* **95**, 116805 (2005).

¹⁹Results related to the filtering of the ambient radiation are beyond the scope of the present paper.

²⁰S. Poran, E. Shimshoni, and A. Frydman (unpublished).